$\times {}^1/_2 = -2.0$ cm^3 mol^{-1}. Thus, for mechanism I, ΔV^* can be expected as $4.7 - 2.0 = 2.7$ cm^3 mol^{-1}. This magnitude is comparable to the experimental ΔV^* values of reactions 2-5. Consequently, mechanism I can be inferred for reactions 2-5.

In the case of reaction 1, ΔV is quite similar to those of reactions 4 and 5. So, if the construction of the transition state were the same as that for reactions 4 and 5, the magnitude of ΔV^* of reaction 1 would also be similar to those of reactions 4 and 5. Thus, the significantly large ΔV^* of reaction 1 seems incompatible with mechanism I. As indicated by Kruse and Taube, a mechanism to form the trigonal-bipyramid transition state may be more appropriate for reaction 1.[11]

Registry No. $Co(en)_2Cl(OH_2)^{2+}$, 82991-06-8.

Contribution from the Department of Chemistry,
Emory University, Atlanta, Georgia 30322

Electronic and Structural Properties of a Reactive Metalloporphyrin with *N*-Oxide Axial Ligands. Crystal and Molecular Structure of Bis(2,6-lutidine *N*-oxide)(tetraphenylporphinato)manganese(III) Perchlorate

CRAIG L. HILL* and MICHAEL M. WILLIAMSON

Received March 19, 1985

Manganese and iron porphyrins are known to catalyze the transfer of oxygen from amine *N*-oxides to hydrocarbon substrates, yet no reactive metalloporphyrin complex containing amine *N*-oxide axial ligands has been structurally characterized to date. An aromatic amine *N*-oxide, 2,6-lutidine *N*-oxide, has been found that forms relatively stable, isolable, soluble, and crystalline metalloporphyrin complexes. Treatment of $Mn^{III}TPP(ClO_4)$ with 2.5 equiv of 2,6-lutidine *N*-oxide in toluene solution followed by the addition of *n*-heptane produces two solvated crystalline modifications of the six-coordinate cationic metalloporphyrin complex bis(2,6-lutidine *N*-oxide)(tetraphenylporphinato)manganese(III) perchlorate (**1**). The magnetic moment (4.9 μ_B at 25 °C), electronic spectrum (λ 325-700 nm), and ^{1}H NMR spectral characteristics from -40 to +60 °C of **1** clearly establish the ground electronic state of the complex to be a d^4 high-spin ($S = 2$) Mn^{III} system in contrast to the Mn porphyrin iodosylbenzene species characterized previously. The magnitudes, alternating signs, and temperature dependencies of the isotropic shifts of the axial *N*-oxide hydrogen atoms indicate clearly that these shifts are primarily contact in origin and arise through a π-delocalization mechanism. Complex **1** crystallizes in the purple-red prism habit as a heptane solvate in the monoclinic space group $C2/c$, with $Z = 8$. The unit cell has $a = 36.644$ (12) Å, $b = 12.3158$ (15) Å, $c = 24.096$ (6) Å, $\alpha = 89.976$ (16)°, $\beta = 95.807$ (23)°, and $\gamma = 90.073$ (20)°. The Mn atom is effectively in the mean plane defined by the 24-atom porphyrin core, and the $d_{Mn-N(Por)}$ values are typical for a $S = 2$ Mn^{III} porphyrin complex. The bonds to the axial oxygen atoms are very long, $d_{Mn-O} = 2.263$ (4) and 2.264 (4) Å, in accord with the axial σ-antibonding character of a d^4 high-spin complex, and the N-O bonds of *N*-oxide moieties are minimally perturbed upon complexation to manganese, $d_{N-O} = 1.331$ (7) and 1.330 (6) Å. Complex **1** is six-coordinate both in the solid state and in solution from -40 to +60 °C.

Introduction

One of the most active areas of chemical research in the last few years has been metalloporphyrin-catalyzed hydrocarbon oxidation processes.[1-6] Synthetic metalloporphyrins have been able to mimic various aspects of the catalytic cycle for hydrocarbon oxidation by the most powerful organic oxidant in nature, cytochrome P-450.[1-7] Several synthetic metalloporphyrin systems as well as cytochrome P-450 itself can catalyze the epoxidation of alkenes and the hydroxylation of alkanes by a source of reduced oxygen such as an iodosylarene, an amine *N*-oxide, or hypochlorite in place of dioxygen and a reducing agent. Substantial experimental evidence suggests that an oxometalloporphyrin 2 electron equivalents more oxidized than the trivalent reactant metalloporphyrin is the actual oxidant that attacks the hydrocarbon substrates both in the enzymic system[7] and in most of the synthetic metalloporphyrin systems.[1-6] The complexes that are formally oxoiron(V) and oxomanganese(V) are kinetically the most competent oxidants for organic substrates that have been encountered in the metalloporphyrin systems examined to date and the only species that attack unactivated alkane C-H bonds at or below 25 °C. Unfortunately, both the formal oxoiron(V) and oxomanganese(V) species are sufficiently reactive that they are not likely to be structurally characterized by X-ray crystallography in the near future. Much progress has been made on the char-

(1) Mn porphyrin based systems: (a) Tabushi, I.; Koga, N. *J. Am. Chem. Soc.* **1979**, *101*, 6456. (b) Tabushi, I.; Koga, N. *Tetrahedron Lett.* **1979**, 3681. (c) Groves, J. T.; Kruper, W. J., Jr.; Haushalter, R. C. *J. Am. Chem. Soc.* **1980**, *102*, 6375. (d) Guilmet, E.; Meunier, B. *Tetrahedron Lett.* **1980**, 4449. (e) Mansuy, D.; Bartoli, J.-F.; Chottard, J.-C.; Lange, M. *Angew. Chem., Int. Ed. Engl.* **1980**, *19*, 909. (f) Chang, C. K.; Ebina, F. *J. Chem. Soc., Chem. Commun.* **1981**, 778. (g) Perrée-Fauvet, M.; Gaudemer, A. *Ibid.* **1981**, 874. (h) Tabushi, I.; Yazaki, A. *J. Am. Chem. Soc.* **1981**, *103*, 7371. (i) Guilmet, E.; Meunier, B. *Nouv. J. Chem.* **1982**, *6*, 511. (j) Groves, J. T.; Takahashi, T. *J. Am. Chem. Soc.* **1983**, *105*, 2073. (k) Groves, J. T.; Watanabe, Y.; McMurry, T. J. *Ibid.* **1983**, *105*, 4489. (l) Collman, J. P.; Kodadek, T.; Raybuck, S. A.; Meunier, B. *Proc. Natl. Acad. Sci. U.S.A.* **1983**, *80*, 7039. (m) Mansuy, D.; Fontecave, M.; Bartoli, J.-F. *J. Chem. Soc., Chem. Commun.* **1983**, 253. (n) Meunier, B.; Guilmet, E.; DeCarvalho, M.-E.; Poilblanc, R. *J. Am. Chem. Soc.* **1984**, *106*, 6668. (o) Collman, J. P.; Brauman, J. I.; Meunier, B.; Raybuck, S. A.; Kodadek, T. *Proc. Natl. Acad. Sci. U.S.A.* **1984**, *81*, 3245.

(2) (a) Schardt, B. C.; Hill, C. L. *J. Am. Chem. Soc.* **1980**, *102*, 6374. (b) Hill, C. L.; Smegal, J. A. *Nouv. J. Chim.* **1982**, *6*, 287. (c) Smegal, J. A.; Hill, C. L. *J. Am. Chem. Soc.* **1983**, *105*, 3515. (d) Hill, C. L.; Smegal, J. A.; Henly, T. J. *J. Org. Chem.* **1983**, *48*, 3277.

(3) Fe porphyrin based systems (see also the many references cited in each and ref 6): (a) Groves, J. T.; Subramanian, D. V. *J. Am. Chem. Soc.* **1984**, *106*, 2177. (b) Groves, J. T.; Myers, R. S. *Ibid.* **1983**, *105*, 5791. (c) Groves, J. T.; Nemo, T. E. *Ibid.* **1983**, *105*, 5786, 6243. (d) Mansuy, D.; Leclaire, J.; Fontecave, M.; Dansette, P. *Tetrahedron* **1984**, 2847. (e) Mansuy, D.; Fontecave, M. *J. Chem. Soc., Chem. Commun.* **1984**, 879.

(4) Cr porphyrin based systems: (a) Groves, J. T.; Kruper, W. J., Jr. *J. Am. Chem. Soc.* **1979**, *101*, 7613. (b) Groves, J. T.; Kruper, W. J., Jr.; Haushalter, R. C.; Butler, W. M. *Inorg. Chem.* **1982**, *21*, 1363.

(5) Powell, M. F.; Pai, E. F.; Bruice, T. C. *J. Am. Chem. Soc.* **1984**, *106*, 3277.

(6) Shannon, P.; Bruice, T. C. *J. Am. Chem. Soc.* **1981**, *103*, 4580. (b) Nee, M. W.; Bruice, T. C. *Ibid.* **1982**, *104*, 6123.

(7) Recent reviews of cytochrome P-450: (a) Guengerich, F. P.; MacDonald, T. L. *Acc. Chem. Res.* **1984**, *17*, 9. (b) Coon, M. J.; White, R. E. "Metal Ion Activation of Dioxygen"; Spiro, T. G., Ed.; Wiley: New York, 1980; Chapter 2. (c) Gunsalus, I. C.; Sligar, S. G. *Adv. Enzymol. Relat. Areas Mol. Biol.* **1978**, *47*, 1. (d) Groves, J. T. *Adv. Inorg. Biochem.* **1979**, *1*, Chapter 4. (e) Chang, C. K.; Dolphin, D. In "Bioorganic Chemistry", van Tamelen, E. E., Ed.; Academic Press: London, 1978; Vol. IV, p 37.

0020-1669/85/1324-3024$01.50/0

acterization of complexes between oxygen atom donors and metalloporphyrins that are immediate precursors to the alkane-functionalizing oxometalloporphyrin forms. For example, iodosylarene[8,9] and hypochlorite[10] complexes of Mn porphyrins have been purified and characterized with varying degrees of rigor. No complex between an oxygen atom donor and a Mn or Fe porphyrin has yet been characterized by X-ray crystallography, however. It has been established primarily by Bruice and co-workers that amine *N*-oxides can transfer oxygen to both Mn and Fe porphyrins to form alkane-activating oxometalloporphyrin complexes.[5,6] One metalloporphyrin complex with aromatic amine *N*-oxide ligands, the high-spin six-coordinate complex bis(pyridine *N*-oxide)(tetraphenylporphyrinato)iron(III) perchlorate, has been prepared and purified. The authors, Reed, Scheidt, and co-workers, characterized this complex by infrared spectroscopy, magnetic susceptibility, and elemental analysis but not by X-ray crystallography.[11] This paper was published prior to the first paper addressing oxygen transfer from amine *N*-oxides catalyzed by metalloporphyrins, and the authors did not discuss the thermal or photochemical decomposition characteristics of this high-spin ferric bis(pyridine *N*-oxide) species. We report here the synthesis, purification, and structural characteristics of a reactive Mn porphyrin complex containing amine *N*-oxide axial ligands, bis(2,6-lutidine *N*-oxide)(tetraphenylporphinato)manganese(III) perchlorate, $[Mn^{III}TPP(2,6\text{-lutNO})_2]^+ClO_4^-$ (**1**).[12] We also report the electronic and structural characteristics of **1** in the solid state and in solution.

Experimental Section

Physical Measurements. Elemental analyses for C, H, and N were performed by Atlanta Microlabs, Inc. The electronic spectra were recorded on a Hewlett-Packard Model 8451A spectrometer. Magnetic susceptibilities were determined in solution by the Evans method.[13] The ^1H NMR spectra were obtained with a Nicolet Model 360-NB 360-MHz spectrometer. The crystallographic data collection and structure solution are described below.

Materials. All reagents and solvents were reagent grade or glass distilled grade from Burdick and Jackson. Reagent grade toluene was purified further by treatment successively with concentrated H_2SO_4, H_2O, NaOH (aq), and H_2O. It was then dried with anhydrous $MgSO_4$ and fractionally distilled from P_2O_5. The deuteriochloroform was "100 atom % D" $CDCl_3$ from Aldrich. The complexes $Mn^{III}TPP(OAc)$,[8] $Mn^{III}TPP(Cl)$,[8] and $Mn^{III}TPP(ClO_4)$[15] were prepared by literature methods.

Synthesis of Bis(2,6-lutidine *N*-oxide)(tetraphenylporphinato)manganese(III) Perchlorate (1). To a stirred solution of 50 mg of $Mn^{III}TPP(ClO_4)$ (0.065 mmol) in 400 mL of toluene at approximately 100 °C was added 2.5 equiv of 2,6-lutidine *N*-oxide. The solution was allowed to cool to room temperature, and then ca. 80 mL of *n*-heptane was carefully layered on top. Two different solvated crystalline modifications of **1** were produced. On the upper walls of the vessel well-formed lustrous deep red-purple prisms accounting for ca. 25% of the starting $Mn^{III}TPP(ClO_4)$ complex were deposited over a period of 4–7 days. One of these crystals was used for the X-ray crystallographic structure determination (vide infra). Most of the remaining **1** crystallized out in a second modification on the lower walls of the vessel after longer periods of time. The ratio of the heptane to both toluene and unligated 2,6-lutidine *N*-oxide had decreased due to slow preferential evaporation of the heptane. This second crystalline modification was dark green needles. Elemental analyses and ^1H NMR spectra of several crops of these green needles indicated that voids in the crystal could be occupied by heptane and/or free 2,6-lutidine *N*-oxide molecules of crystallization.[14] Characterization of the electronic and ^1H NMR spectral properties of **1** is described in the Results and Discussion. Anal. Calcd for $C_{65}H_{62}ClMnN_6O_6$, $[MnTPP(2,6\text{-lutNO})_2]ClO_4 \cdot C_7H_{16}$: C, 70.11; H, 5.61; N, 7.55. Found: C, 70.04; H, 5.05; N, 7.40.

X-ray Crystallography. Data Collection. The X-ray diffractometer, computer hardware, and software used in crystallographic structure determination at Emory were described previously.[15] A purple-red crystal of the prism habit was attached to the end of a glass fiber with epoxy cement. The fiber was then mounted on a goniometer head, and then the head was placed on the Syntex $P2_1$ diffractometer. After the crystal was centered, accurate cell dimensions were determined by least-squares refinement of 15 centered reflections (θ = 6.29–11.93°; λ(Mo K$\bar{\alpha}$) = 0.71069 Å). The θ–2θ scan method with a variable scan rate of 2.02–29.3° min^{-1} (scan time/background = 1) was used. Intensity measurements of 3 standards every 97 reflections showed no evidence of crystal deterioration. Intensities (2θ = 4.2–50.0°) were measured for 9583 reflections, of which 6134 unique reflections were observed ($F \geq 2.5\sigma(F)$). Crystal and data collection parameters are summarized in Table I.

Structure Solution and Refinement. The computer hardware and software for data refinement and structure solution were described previously.[15] The data exhibited the systematic absences hkl, $h + k = 2n + 1$, and $h0l$, $l = 2n + 1$, suggesting Cc or $C2/c$ as the only likely space groups. The statistical distribution of the normalized structure factors, E's, strongly indicated a centric space group. The structure was solved in the only centric space group of the reasonable choices, $C2/c$. The position of the Mn atom was located by conventional Patterson synthesis. All non-hydrogen atoms were located in subsequent difference Fourier syntheses. A disordered *n*-heptane molecule of crystallization was located along a twofold axis, and carbon atoms were placed at the highest electron density peaks. The perchlorate anion was also disordered. The best resolution of the ClO_4^- had two oxygens of unit occupancy and four oxygens of $^1/_2$ occupancy. All non-hydrogen atoms except the carbon atoms of heptane were allowed to refine anisotropically. All the hydrogens except the 2,6-methyl hydrogens were placed in their calculated positions and allowed to refine independently. In the latter stages of refinement they were fixed. The 2,6-methyl hydrogens were allowed to "ride" on their parent carbons (C–H = 0.96 Å; $U_{iso}(H) = 1.2[U_{ij}(C)]$). The final electron density difference map was clean except for a positive peak (0.63 e $Å^{-3}$) 1.34 Å from a carbon atom of the heptane. Block-cascade matrix least-squares refinement of 697 variables gave final agreement factors of $R = 0.0908$ and $R_w = 0.0953$, where $R = \sum||F_o| - |F_c||/|F_o|$ and $R_w = [\sum w(|F_o| - |F_c|)^2/\sum w|F_o|^2]^{1/2}$. The GOF was 1.407; GOF = $(\sum w(|F_o| - |F_c|)^2/n_o - n_v)^{1/2}$. On the last cycle of the least-squares refinement the ratio of the maximum shift to the estimated standard deviation was −0.161. The data were corrected for Lorentz–polarization; no adsorption correction was performed. A weighing

Table I. Crystal and Data Collection Parameters for $[Mn^{III}TPP(2,6\text{-lutNO})_2]^+ClO_4^-$ (**1**)

(A) Crystal Parameters at 25 °C[a,b]

space group: $C2/c$ (No. 15)	dimens: 0.5 × 0.3 × 0.2 mm
$Z = 8$	$V = 10818.9$ (46) Å^3
$a = 36.644$ (12) Å	fw = 1113.638
$b = 12.3158$ (15) Å	$d_{calcd} = 1.31$ g cm^{-3}
$c = 24.096$ (6) Å	$d_{obsd} = 1.33$ g cm^{-3}
$\alpha = 89.976$ (16)°	$\mu_{calcd} = 3.7$ cm^{-1}
$\beta = 95.807$ (23)°	color: purple-red
$\gamma = 90.073$ (20)°	

(B) Data Measurement

radiation: Mo K$\bar{\alpha}$ (λ = 0.71069 Å)
monochromator: highly oriented graphite ($2\theta_M$ = 12.2°), perpendicular mode, assumed 50% perfect
reflcns measd: $\pm h, +k, +l$
2θ range: 4.2–50.0°
scan type: θ–2θ
scan speed (θ): 2.02 (min), 29.3 (max) deg/min
scan time/bkgd: 1
reflcns collected (including stds): 10648
unique reflcns used in least-squares refinement: 6134 with $F_o > 2.5\sigma F_o$
std reflcns: 3, measd every 97 reflcns

[a] Unit cell parameters were derived by a least-squares fit of 15 centered reflections with θ between 6.29 and 11.93°. [b] In this and all subsequent tables the esd's of all parameters are given in parentheses for the least significant digit(s) given.

(8) Smegal, J. A.; Schardt, B. C.; Hill, C. L. *J. Am. Chem. Soc.* **1983**, *105*, 3510.
(9) Smegal, J. A.; Hill, C. L. *J. Am. Chem. Soc.* **1983**, *105*, 2920.
(10) Bartolini, O.; Meunier, B. *J. Chem. Soc., Chem. Commun.* **1983**, 1364.
(11) Mashiko, T.; Kastner, M. E.; Spartalian, K.; Scheidt, W. R.; Reed, C. A. *J. Am. Chem. Soc.* **1978**, *100*, 6354.
(12) Abbreviations: TPP = dianion of 5,10,15,20-tetraphenylporphyrin; pyrNO = pyridine *N*-oxide; 2,6-lutNO = 2,6-lutidine *N*-oxide; acac = acetylacetonate anion ligand.
(13) Evans, D. F. *J. Chem. Soc.* **1959**, 2003.
(14) Preliminary crystallographic information on a representative crystal of the second or green-needle modification was obtained. For $[Mn^{III}TPP(2,6\text{-lutNO})_2]^+ClO_4^- \cdot 1.0\ C_6H_5CH_3$, a crystal 0.88 × 0.10 × 0.16 mm in monoclinic space group $P2_1/c$ had $a = 20.3851$ (134) Å, $b = 12.2073$ (42) Å, $c = 24.0310$ (250) Å, $\beta = 113°$, cell volume 5501.88 (7.24) Å^3, and $Z = 4$. The toluene molecules of crystallization were severely disordered.
(15) Hill, C. L.; Williamson, M. M. *Inorg. Chem.* **1985**, *24*, 2836.

Table II. Atom Coordinates ($\times 10^4$) and Temperature Factors ($Å^2 \times 10^3$)

atom	x	y	z	U^a	atom	x	y	z	U^a
Mn	1756 (1)	1051 (1)	2756 (1)	31 (1)	C(29)	3339 (2)	1108 (5)	4729 (3)	52 (2)
O(1a)	1816 (1)	2879 (3)	2745 (2)	50 (2)	C(30)	3539 (2)	158 (6)	4691 (3)	55 (2)
O(1b)	1769 (1)	−786 (4)	2774 (2)	58 (2)	C(31)	3408 (2)	−630 (5)	4316 (3)	47 (2)
N(2a)	1614 (1)	3628 (4)	2965 (2)	40 (2)	C(32)	3083 (2)	−478 (5)	3982 (3)	40 (2)
N(2b)	1553 (2)	−1452 (4)	2452 (2)	54 (2)	C(33)	1033 (1)	1662 (5)	4337 (2)	38 (2)
N(1)	2290 (1)	1027 (4)	2665 (2)	33 (1)	C(34)	884 (2)	2700 (6)	4348 (3)	53 (2)
N(2)	1867 (1)	974 (4)	3587 (2)	33 (1)	C(35)	679 (2)	3007 (7)	4790 (3)	65 (3)
N(3)	1221 (1)	1098 (4)	2842 (2)	35 (2)	C(36)	630 (2)	2258 (7)	5204 (3)	67 (3)
N(4)	1638 (1)	1096 (4)	1928 (2)	30 (1)	C(37)	775 (2)	1256 (8)	5187 (3)	72 (3)
C(1)	2449 (2)	1229 (4)	2186 (2)	32 (2)	C(38)	981 (2)	954 (6)	4757 (3)	53 (2)
C(2)	2839 (2)	1083 (5)	2288 (2)	37 (2)	C(39)	625 (2)	541 (5)	1492 (2)	40 (2)
C(3)	2912 (2)	790 (5)	2827 (2)	38 (2)	C(40)	486 (2)	1290 (6)	1097 (3)	55 (2)
C(4)	2567 (1)	772 (4)	3070 (2)	34 (2)	C(41)	160 (2)	1018 (8)	751 (3)	77 (3)
C(5)	2537 (1)	632 (4)	3633 (2)	31 (2)	C(42)	−17 (2)	100 (8)	812 (3)	72 (3)
C(6)	2204 (2)	772 (4)	3880 (2)	34 (2)	C(43)	116 (2)	−640 (7)	1210 (3)	73 (3)
C(7)	2170 (2)	823 (5)	4465 (2)	42 (2)	C(44)	435 (2)	−407 (6)	1549 (3)	58 (3)
C(8)	1819 (2)	1090 (5)	4527 (2)	42 (2)	C(3a)	1727 (2)	4023 (5)	3484 (3)	54 (2)
C(9)	1626 (2)	1170 (5)	3982 (2)	36 (2)	C(9a)	2075 (2)	3630 (6)	3757 (3)	77 (3)
C(10)	1252 (2)	1368 (5)	3867 (2)	37 (2)	C(4a)	1514 (3)	4802 (6)	3706 (3)	75 (4)
C(11)	1063 (2)	1283 (5)	3329 (2)	40 (2)	C(5a)	1194 (3)	5182 (7)	3403 (4)	92 (4)
C(12)	672 (2)	1198 (7)	3220 (3)	58 (3)	C(6a)	1100 (2)	4797 (6)	2884 (4)	73 (3)
C(13)	598 (2)	966 (7)	2678 (3)	57 (3)	C(7a)	1309 (2)	4010 (5)	2655 (3)	54 (2)
C(14)	936 (2)	888 (5)	2432 (2)	38 (2)	C(8a)	1229 (2)	3617 (6)	2076 (3)	72 (3)
C(15)	968 (2)	780 (4)	1862 (2)	36 (2)	C(3b)	1247 (2)	−1850 (6)	2659 (4)	71 (3)
C(16)	1299 (2)	920 (4)	1635 (2)	34 (2)	C(9b)	1170 (3)	−1546 (8)	3218 (4)	98 (4)
C(17)	1329 (2)	1075 (5)	1050 (2)	42 (2)	C(4b)	1014 (3)	−2523 (7)	2313 (5)	100 (4)
C(18)	1684 (2)	1365 (5)	998 (2)	39 (2)	C(5b)	1099 (3)	−2796 (8)	1797 (6)	102 (5)
C(19)	1882 (2)	1350 (4)	1540 (2)	31 (2)	C(6b)	1414 (3)	−2407 (7)	1609 (4)	91 (4)
C(20)	2262 (2)	1463 (4)	1660 (2)	31 (2)	C(7b)	1647 (2)	−1748 (5)	1939 (3)	62 (3)
C(21)	2493 (2)	1762 (4)	1205 (2)	32 (2)	C(8b)	2018 (3)	−1434 (7)	1804 (4)	99 (4)
C(22)	2719 (2)	2665 (5)	1265 (3)	42 (2)	Cl	798 (1)	7318 (3)	4628 (2)	148 (2)
C(23)	2960 (2)	2888 (5)	872 (3)	52 (2)	O(1)	955 (5)	6523 (12)	4416 (5)	388 (10)
C(24)	2976 (2)	2221 (6)	421 (3)	50 (2)	O(2)	778 (5)	6974 (15)	5172 (5)	311 (11)
C(25)	2750 (2)	1340 (6)	346 (3)	51 (2)	O(3)	471 (7)	7767 (24)	4559 (9)	295 (16)
C(26)	2509 (2)	1112 (5)	737 (2)	40 (2)	O(3′)	607 (5)	7391 (24)	4133 (9)	229 (14)
C(27)	2882 (2)	460 (5)	4019 (2)	35 (2)	O(4)	1171 (5)	8179 (20)	4749 (9)	195 (12)
C(28)	3014 (2)	1243 (5)	4394 (3)	43 (2)	O(4′)	804 (7)	8272 (18)	4561 (17)	355 (23)

[a] Equivalent isotropic U defined as one-third of the trace of the orthogonalized U tensor.

scheme, utilizing weights of the form $w = [\sigma^2(F_o) + |g|F_o^2]^{-1}$ (where $g = 0.0036$), was implemented as a result of an analysis of the data set as a function of F_o, 2θ, and hkl. Scattering factors were those for neutral atoms;[16] final positional and thermal parameters are given in Table II.

Selected bond lengths and angles are enumerated in Tables III and IV, respectively, in the Results and Discussion. The remaining structural information including anisotropic thermal parameters, hydrogen atom coordinates, other bonds and angles, and structure factors are included in the supplementary material.

Results and Discussion

Synthesis and Isolation of Bis(amine *N*-oxide)manganese Porphyrin Complexes. Both Fe and Mn porphyrins catalyze the transfer of oxygen from amine *N*-oxides to hydrocarbon substrates.[5,6] Both aromatic[17] and aliphatic[5,6] amine *N*-oxides transfer oxygen although the latter are more reactive than the former. Bruice has shown that at least within the *N*,*N*-dimethylaniline *N*-oxide series the presence of electron-withdrawing substituents on the phenyl ring greatly enhances the kinetic ability of the *N*-oxide to transfer oxygen to the metalloporphyrin and hence to substrate.[5] Our goal in this work was to select an amine *N*-oxide that formed sufficiently stable complexes with either iron or manganese porphyrins that the porphyrin complexes could be prepared and manipulated extensively at ambient laboratory temperature. That is, the decomposition of the metalloporphyrin axially ligated by *N*-oxide ligands to the formal oxometal(V) species was slow at 25 °C. We also sought an *N*-oxide that would render the corresponding metalloporphyrin complexes both soluble and crystalline. The compound 2,6-lutidine *N*-oxide proved to impart the above properties when complexes to Mn porphyrins. Bis(2,6-lutidine *N*-oxide) complexes could be prepared in high yield by adding 2.5 equiv of the *N*-oxide to $Mn^{III}TPP(Y)$ complexes (Y = ClO_4^-, BF_4^-, or other weakly coordinating anionic axial ligand) in a chlorine-free nonpolar organic solvent. The product complexes formed in high yield in toluene solution. Two crystalline modifications of the bis(2,6-lutidine *N*-oxide)(tetraphenylporphinato)manganese(III) perchlorate complex (**1**) could be obtained, one of which produced diffraction-quality single crystals. The coordination form of **1** in solution is addressed below.

Ground-State Electronic Structure of 1. Complex **1** is only one elementary process, the cleavage of the N–O bond, away from an alkane-activating oxometalloporphyrin species. Complex **1** is also the only such metalloporphyrin that has been throughly characterized by X-ray crystallography. As a consequence, the structural and electronic features of the metal and the axial *N*-oxide units in **1** warrant careful scrutiny.

Magnetic Susceptibility and Electronic Spectrum of 1. The magnetic moment, μ_{eff}, of **1** in solution at 25 °C determined by the Evans method was the same as for the well-characterized conventional Mn(III) high-spin d^4 complex $Mn^{III}TPP(Cl)$, 4.9 μ_B.[13,18] This value is the same within experimental error as the spin-only value for an $S = 2$ system and indicates that there is very little spin–orbit coupling associated with the d electrons of **1**. The electronic spectra of **1** and representative Mn^{III}, Mn^{IV}, and Mn^{V} porphyrin complexes over the spectral range of λ 325–700 nm are compared in Figure 1. All spectra were obtained in the same solvent (toluene) at the same concentration and at the same temperature. Earlier we reported the preparation, purification, and characterization including the X-ray crystal structures of both the highly reactive dimeric Mn^{IV} complex $[N_3Mn^{IV}TPP]_2O$[19] and the unreactive nitrido complex $NMn^{V}T$-

(16) Cromer, D. T.; Waber, J. T. "International Tables for X-ray Crystallography"; Kynoch Press: Birmingham, England, 1974; Vol. IV, Table 2.2B.

(17) Hill, C. L.; Brown, R., unpublished results.

(18) Behere, B. V.; Mitra, S. *Inorg. Chem.* **1980**, *19*, 992.

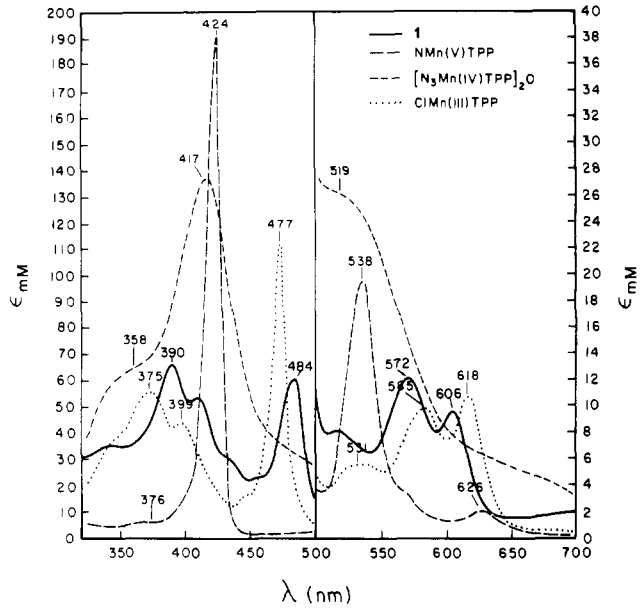

Figure 1. Electronic spectra of **1** and representative Mn^{III}, Mn^{IV}, and Mn^{V} porphyrin complexes: (—) **1**; (—) $NMn^{V}TPP$; (---) $[N_3Mn^{IV}TPP]_2O$; (···) $ClMn^{III}TPP$. The spectrum of $NMn^{V}TPP$ for λ 325–500 nm is half-scale. All spectra were recorded as approximately 1.0 mM solutions in toluene at 25 °C.

PP[20] whose electronic spectra appear in Figure 1. The ultraviolet–visible spectra of monomeric Mn^{IV} porphyrin complexes are very similar to those of the dimeric Mn^{IV} complexes such as $[N_3Mn^{IV}TPP]_2O$.[21] It is apparent upon examination of Figure 1 that the electronic spectrum of **1** is similar to that of the authentic Mn^{III} complex $Mn^{III}TPP(Cl)$ and quite distinct from those of the Mn^{IV} and Mn^{V} complexes. Little further information about the electronic structure of **1** can be inferred unequivocally from the relative intensities of the split Soret and other absorption bands. Most of the bands in the electronic spectrum of **1** are primarily $\pi-\pi^*$ in origin, but some can be attributed, albeit with less certainty, to charge-transfer transitions of the type a_{1u}(porphyrin ring π), a_{2u}(porphyrin ring π) → e_g(d_π of Mn).[22]

^{1}H NMR Spectra of 1. The ^{1}H NMR spectra of **1** not only substantiate the assignment of an $S = 2$ Mn^{III} atom in **1** derived from the magnetic susceptibility and electronic spectra above but also supply information about the coordination form of the complex in solution and the magnitude and character of the delocalization of d-orbital unpaired spin density onto the axial *N*-oxide ligands. The ^{1}H NMR spectra of **1** over the temperature range of +60 to −40 °C are illustrated in Figure 2. All proton assignments, indicated on the figure, could be ascertained readily from chemical shifts, line widths, and integrations. Both the chemical shifts and line widths of the porphyrin phenyl and β-pyrrole hydrogens of **1** are similar to those of five-coordinate $S = 2$ Mn^{III} porphyrins, $Mn^{III}(por)(X)$,[23] six-coordinate $S = 2$ Mn^{III} porphyrins, $Mn^{III}(Por)(L)(X)$,[23] and six-coordinate $S = 2$ Mn^{III} porphyrin cations, $[Mn^{III}(por)(L)_2]^+X^-$, where L = DMF, 1-methylimidazole.[15] The chemical shifts and line widths of **1** are distinct, however, from those of Mn^{II},[24] low-spin ($S = 1$) Mn^{III},[25] Mn^{IV},[8,26] and Mn^{V}[20] porphyrin complexes. The isotropic shifts of the hydrogens on **1** are plotted as a function of reciprocal temperature in Figure 3. The isotropic shifts are referenced to the diamagnetic complex $Zn^{II}TPP$. The possibility of thermal decomposition of **1** via N–O bond cleavage or other mechanisms at the higher temperatures used to record the ^{1}H NMR spectra was addressed by rerecording the 20 °C spectra after the 60 °C spectra had been obtained. Such control experiments indicated that the degree of thermal decomposition of **1** over the duration of the entire NMR data acquisition

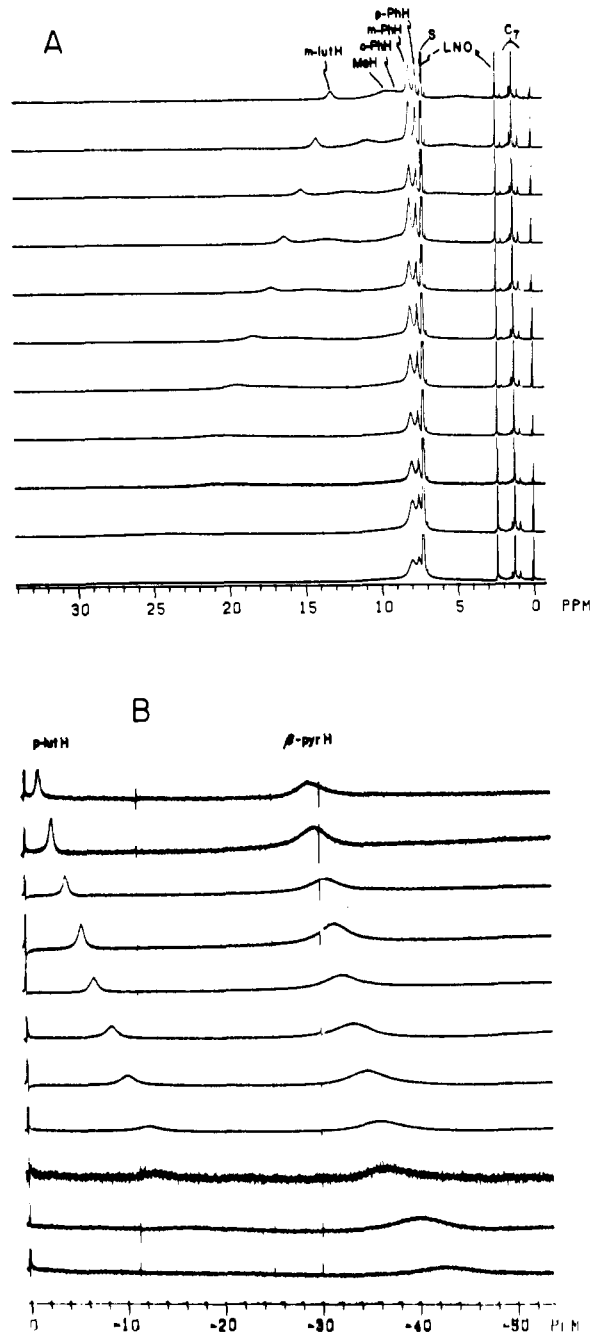

Figure 2. ^{1}H NMR spectra of **1** from +60 (top of A and B) to −40 °C (bottom of A and B) at 10 °C intervals: (A) 0 to +30 ppm; (B) 0 to −50 ppm. The sample used was the green-needle crystalline modification that contained both free (nonligated) 2,6-lutidine *N*-oxide (designated LNO on figure) and free heptane (designated C_7 on figure). The peak marked S for solvent is the trace of $CHCl_3$ present. All spectra were recorded on the same sample (0.024 M in "100 atom % D" deuteriochloroform). All proton assignments for **1** are labeled on the top (+60 °C) spectra. The ortho Ph protons were not clearly resolved in most of the spectra.

(19) Schardt, B. C.; Hollander, F. J.; Hill, C. L. *J. Am. Chem. Soc.* **1982**, *104*, 3964.
(20) Hill, C. L.; Hollander, F. J. *J. Am. Chem. Soc.* **1982**, *104*, 7318. The complex actually submitted to structural analysis by X-ray crystallography was not the tetraphenylporphinato or TPP derivative but the tetrakis(*p*-methoxyphenyl)porphinato derivative.
(21) (a) Camenzind, M. J.; Hollander, F. J.; Hill, C. L. *Inorg. Chem.* **1982**, *21*, 4301. (b) Camenzind, M. J.; Hollander, F. J.; Hill, C. L. *Ibid.* **1983**, *22*, 3776.
(22) Gouterman, M. In "The Porphyrins"; Dolphin, D., Ed.; Academic Press: New York, 1978; Vol. III, Part A, Chapter 1.
(23) La Mar, G. N.; Walker, F. A. *J. Am. Chem. Soc.* **1975**, *97*, 5103.
(24) Hansen, A. P. M.S. Thesis, University of Iowa, 1982.
(25) Hansen, A. P.; Goff, H. M. *Inorg. Chem.* **1984**, *23*, 4519.
(26) Camenzind, M. J. Ph.D. Thesis, University of California, Berkeley, CA, 1983. Schardt, B. C. Ph.D. Thesis, University of California, Berkeley, CA, 1984.

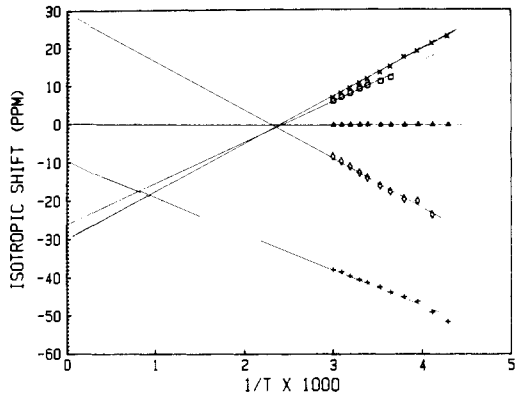

Figure 3. ^{1}H NMR Curie law plot of **1** from +60 to −40 °C (concentration 0.024 M in "100 atom % D" deuteriochloroform): (×) lutidine methyl protons; (□) meta lutidine protons; (△) para phenyl (TPP) protons; (◇) para lutidine protons; (+) β-pyrrole protons. The meta phenyl (TPP) protons have been omitted for clarity as they have very small isotropic shifts and overlap with the para phenyl protons; the ortho phenyl protons were not clearly resolved in most of the spectra. Isotropic shifts are defined relative to a diamagnetic Zn^{II}TPP standard.

sequence was negligible. The slight curvature in some of the lines in Figure 3, particularly that of the β-pyrrole hydrogens, could be due in part to the difficulty of assigning exact values for the chemical shifts on such broad peaks at the lower temperatures. This problem is most acute for the β-pyrrole hydrogens because these hydrogens are closest to the paramagnetic manganese atom and the ^{1}H relaxation mechanisms in **1**, as for other $S = 2$ Mn^{III} porphyrin complexes, are primarily dipolar in nature.[27]

The isotropic shifts for the porphyrin phenyl hydrogens of **1** are small, ruling out appreciable dipolar contributions to these shifts. The β-pyrrole hydrogen chemical shifts are far upfield from Me_4Si, consistent with the $d_{x^2-y^2}$ orbital being empty and the d_{xz} and d_{yz} orbitals being partially filled. The line width of the β-pyrrole resonance rules out any appreciable low-spin ($S = 1$) Mn^{III} character to **1**, as the β-pyrrole line widths in $S = 1$ Mn^{III} porphyrin complexes are quite distinct and very sharp.[25] There is an absence of appreciable curvature in the ^{1}H NMR Curie law plot of **1** (Figure 3). We previously demonstrated that cationic six-coordinate $S = 2$ Mn^{III} porphyrin complexes could give rise to either linear or nonlinear Curie law plots. Nonlinearity, although it could arise for several reasons, is most likely to arise in these d^4 high-spin systems from changes in axial ligation. That is, different coordination forms involving the axial ligands predominate at different temperatures.[15] The absence of curvature in the Curie law plot of **1** in deuteriochloroform solution suggests strongly that one coordination form of the complex, undoubtedly the six-coordinate form with two *N*-oxide axial ligands that exists in the solid state (vide infra), is the principal form in this solvent over the entire experimental temperature range (−40 to +60 °C). Furthermore, the linearity of this plot indicates that there is no change of spin state, dynamic valence isomerization, or other major perturbation of the ground-state electronic structure of **1** in solution over this temperature range. The origin of the nonzero intercepts at $T^{-1} = 0$ on the Curie law plot is uncertain. Such nonzero intercepts have been attributed for both low-spin Fe^{III} and high-spin Mn^{III} porphyrin complexes to a second-order Zeeman interaction.[23,28,29] The magnitude, alternating signs, and temperature dependencies of the isotropic shifts of the axial 2,6-lutidine *N*-oxide hydrogens demonstrate that these shifts are primarily contact in origin and arise through π-delocalization mechanisms.[30] The 2,6-lutidine moiety is an alternate ligand system; similar alternate ligand systems containing phenyl groups have been used as diagnostic probes for contact shifts previously.[30,31] The *o*-methyl hydrogens have a direct contact interaction with the π-spin density at the ortho position of the lutidine moiety via hyperconjugation.[32]

Table III. Selected Bond Lengths (Å)

Mn–O(1a)	2.263 (4)	Mn–O(1b)	2.264 (4)
Mn–N(1)	1.991 (4)	Mn–N(2)	2.004 (4)
Mn–N(3)	1.991 (4)	Mn–N(4)	1.999 (4)
O(1a)–N(2a)	1.330 (6)	O(1b)–N(2b)	1.331 (7)
N(2a)–C(3a)	1.365 (8)	N(2a)–C(7a)	1.364 (8)
N(2b)–C(3b)	1.362 (10)	N(2b)–C(7b)	1.368 (10)
N(1)–C(1)	1.367 (7)	N(1)–C(4)	1.373 (7)
N(2)–C(6)	1.382 (7)	N(2)–C(9)	1.386 (7)
N(3)–C(11)	1.380 (7)	N(3)–C(14)	1.387 (7)
N(4)–C(16)	1.383 (7)	N(4)–C(19)	1.391 (7)
C(1)–C(2)	1.438 (8)	C(1)–C(20)	1.408 (7)
C(2)–C(3)	1.348 (8)	C(3)–C(4)	1.445 (8)
C(4)–C(5)	1.384 (8)	C(5)–C(6)	1.419 (8)
C(5)–C(27)	1.507 (7)	C(6)–C(7)	1.431 (8)
C(7)–C(8)	1.352 (9)	C(8)–C(9)	1.431 (8)
C(9)–C(10)	1.393 (8)	C(10)–C(11)	1.410 (8)
C(10)–C(33)	1.496 (8)	C(11)–C(12)	1.431 (8)
C(12)–C(13)	1.338 (9)	C(13)–C(14)	1.429 (8)
C(14)–C(15)	1.398 (8)	C(15)–C(16)	1.389 (8)
C(15)–C(39)	1.496 (7)	C(16)–C(17)	1.440 (8)
C(17)–C(18)	1.366 (8)	C(18)–C(19)	1.427 (7)
C(19)–C(20)	1.400 (7)	C(3a)–C(4a)	1.381 (11)
C(3a)–C(9a)	1.456 (10)	C(5a)–C(6a)	1.348 (13)
C(4a)–C(5a)	1.399 (14)	C(7a)–C(8a)	1.478 (10)
C(6a)–C(7a)	1.385 (11)	C(3b)–C(4b)	1.402 (13)
C(3b)–C(9b)	1.452 (14)	C(5b)–C(6b)	1.368 (16)
C(4b)–C(5b)	1.354 (18)	C(7b)–C(8b)	1.480 (13)
C(6b)–C(7b)	1.370 (11)		

X-ray Crystal Structure of 1. A representative crystal of the red prism crystalline modification was submitted to analysis by X-ray crystallography. An ORTEP[33] and numbering diagram for the bis(2,6-lutidine *N*-oxide)(tetraphenylporphinato)manganese(III) cation is shown in Figure 4. The unit cell is sufficiently crowded that the porphyrin phenyl groups in addition to the perchlorate counterion and the heptane molecule of crystallization have been omitted for clarity.

The molecules of **1** pack tightly in the unit cell, and no large channels exist. The perchlorate anion is well separated from the cation ($d_{Mn-Cl} = 9.775$ Å). The bis(2,6-lutidine *N*-oxide)(tetraphenylporphinato)manganese(III) cation has no crystallographically imposed symmetry; every atom is crystallographically unique. The 24-atom porphyrin core shows some S_4 ruffling, a common structural feature displayed by metalloporphyrins.[15,34] The Mn atom is effectively in the mean plane defined by the 24-atom core (0.0006 Å away from this center point) and the mean plane defined by the four porphyrin nitrogen atoms (0.0028 Å

(27) La Mar, G. N.; Walker, F. A. *J. Am. Chem. Soc.* **1973**, *95*, 6950.
(28) Jesson, J. P. In "NMR of Paramagnetic Molecules"; La Mar, G. N., Horrocks, W. D., Holm. R. H., Eds.; Academic Press: New York, 1973; Chapter 1.
(29) Goff and Hansen had observed large nonzero intercepts on ^{13}C NMR Curie law plots of $S = 2$ Mn^{III} porphyrin complexes; cf.: Goff, H. M.; Hansen, A. P. *Inorg. Chem.* **1984**, *23*, 321.
(30) Horrocks, W. D., Jr. In ref 28, Chapter 4.
(31) (a) Holm, R. H.; Phillips, W. D.; Averill, B. A.; Mayerle, J. J.; Herskovitz, T. *J. Am. Chem. Soc.* **1974**, *96*, 2109. (b) Eaton, D. R.; Josey, A. D.; Phillips, W. D.; Benson, R. E. *J. Chem. Phys.* **1962**, *37*, 347. (c) Eaton, D. R.; Josey, A. D.; Benson, R. E. *J. Am. Chem. Soc.* **1967**, *89*, 4040. (d) Eaton, D. R.; Josey, A. D.; Benson, R. E.; Phillips, W. D. *Ibid.* **1962**, *84*, 4100. (e) Parks, J. E.; Holm, R. H. *Inorg. Chem.* **1968**, *7*, 1408.
(32) (a) McConnell, H. M. *J. Chem. Phys.* **1956**, *24*, 764. (b) McLachlan, A. D. *Mol. Phys.* **1958**, *1*, 233.
(33) Johnson, C. K. *Oak Ridge Natl. Lab.*, [*Rep.*] *ORNL* (*U.S.*) **1965**, *ORNL-3794*.
(34) Scheidt, W. R. In "The Porphyrins"; Dolphin, D., Ed.; Academic Press: New York, 1978; Vol. III, Part A, Chapter 10 and references cited therein.
(35) Scavnicar, S.; Matkovic, B. *Acta Crytstallogr., Sect. B: Struct. Crystallogr. Cryst. Chem.* **1969**, *B25*, 2046.
(36) Lee, J. D.; Brown, D. S.; Melsom, B. G. A. *Acta Crystallogr., Sect. B: Struct. Crystallogr. Cryst. Chem.* **1969**, *B25*, 1378.
(37) Sager, R. S.; Watson, W. H. *Inorg. Chem.* **1969**, *8*, 308.
(38) Sagar, R. S.; Watson, W. H. *Inorg. Chem.* **1968**, *7*, 1358.
(39) Horrocks, W. D., Jr.; Templeton, D. H.; Zalkin, A. *Inorg. Chem.* **1968**, *7*, 1552.
(40) Blom, E. A.; Penfold, B. R.; Robinson, W. T. *J. Chem. Soc. A* **1969**, 913.

Table IV. Selected Bond Angles (deg)

O(1a)-Mn-O(1b)	173.2 (2)	O(1a)-Mn-N(1)	85.2 (2)
O(1b)-Mn-N(1)	88.1 (2)	O(1a)-Mn-N(2)	92.8 (2)
O(1b)-Mn-N(2)	86.2 (2)	N(1)-Mn-N(2)	90.3 (2)
O(1a)-Mn-N(3)	94.0 (2)	O(1b)-Mn-N(3)	92.7 (2)
N(1)-Mn-N(3)	179.1 (2)	N(2)-Mn-N(3)	90.0 (2)
O(1a)-Mn-N(4)	88.4 (2)	O(1b)-Mn-N(4)	92.8 (2)
N(1)-Mn-N(4)	90.3 (2)	N(2)-Mn-N(4)	178.7 (2)
N(3)-Mn-N(4)	89.4 (2)	Mn-O(1a)-N(2a)	128.8 (3)
Mn-O(1b)-N(2b)	126.5 (3)	O(1a)-N(2a)-C(3a)	118.9 (5)
O(1a)-N(2a)-C(7a)	118.7 (5)	C(3a)-N(2a)-C(7a)	122.3 (5)
O(1b)-N(2b)-C(3b)	118.1 (6)	O(1b)-N(2b)-C(7b)	120.0 (6)
C(3b)-N(2b)-C(7b)	121.9 (6)	Mn-N(1)-C(1)	126.7 (3)
Mn-N(1)-C(4)	126.3 (4)	C(1)-N(1)-C(4)	107.0 (4)
Mn-N(2)-C(6)	126.9 (4)	Mn-N(2)-C(9)	126.8 (3)
C(6)-N(2)-C(9)	186.2 (4)	Mn-N(3)-C(11)	126.7 (3)
Mn-N(3)-C(14)	126.7 (4)	C(11)-N(3)-C(14)	106.6 (4)
Mn-N(4)-C(16)	126.6 (4)	Mn-N(4)-C(19)	126.2 (3)
C(16)-N(4)-C(19)	107.2 (4)	N(1)-C(1)-C(2)	109.5 (4)
N(1)-C(1)-C(20)	125.9 (5)	C(2)-C(1)-C(20)	124.4 (5)
C(1)-C(2)-C(3)	107.2 (5)	C(2)-C(3)-C(4)	107.3 (5)
N(1)-C(4)-C(3)	108.9 (5)	N(1)-C(4)-C(5)	126.7 (5)
C(3)-C(4)-C(5)	124.0 (5)	C(4)-C(5)-C(6)	123.6 (5)
C(4)-C(5)-C(27)	118.5 (5)	C(6)-C(5)-C(27)	117.5 (5)
N(2)-C(6)-C(5)	124.7 (5)	N(2)-C(6)-C(7)	109.5 (5)
C(5)-C(6)-C(7)	125.6 (5)	C(6)-C(7)-C(8)	107.4 (5)
C(7)-C(8)-C(9)	107.7 (5)	N(2)-C(9)-C(8)	109.2 (5)
N(2)-C(9)-C(10)	125.3 (5)	C(8)-C(9)-C(10)	125.5 (5)
C(9)-C(10)-C(11)	123.6 (5)	C(9)-C(10)-C(33)	118.9 (5)
C(11)-C(10)-C(33)	117.5 (5)	N(3)-C(11)-C(10)	125.6 (5)
N(3)-C(11)-C(12)	109.3 (5)	C(10)-C(11)-C(12)	124.3 (5)
C(11)-C(12)-C(13)	107.1 (6)	C(12)-C(13)-C(14)	108.7 (5)
N(3)-C(14)-C(13)	108.2 (5)	N(3)-C(14)-C(15)	125.9 (5)
C(13)-C(14)-C(15)	125.2 (5)	C(14)-C(15)-C(16)	122.5 (5)
C(14)-C(15)-C(39)	117.1 (5)	C(16)-C(15)-C(39)	120.3 (5)
N(4)-C(16)-C(15)	126.4 (5)	N(4)-C(16)-C(17)	109.0 (5)
C(15)-C(16)-C(17)	123.9 (5)	C(16)-C(17)-C(18)	107.0 (5)
C(17)-C(18)-C(19)	108.2 (5)	N(4)-C(19)-C(18)	108.6 (5)
N(4)-C(19)-C(20)	125.0 (5)	C(18)-C(19)-C(20)	126.1 (5)
C(1)-C(20)-C(19)	123.3 (5)	C(1)-C(20)-C(21)	116.7 (5)
C(19)-C(20)-C(21)	119.8 (4)	C(20)-C(21)-C(22)	119.8 (5)
C(20)-C(21)-C(26)	121.9 (5)	N(2a)-C(3a)-C(9a)	117.8 (6)
N(2a)-C(3a)-C(4a)	118.1 (6)	C(9a)-C(3a)-C(4a)	124.0 (7)
C(3a)-C(4a)-C(5a)	120.5 (7)	C(4a)-C(5a)-C(6a)	119.3 (9)
C(5a)-C(6a)-C(7a)	121.1 (8)	N(2a)-C(7a)-C(6a)	118.6 (6)
N(2a)-C(7a)-C(8a)	118.5 (6)	C(6a)-C(7a)-C(8a)	122.8 (7)
N(2b)-C(3b)-C(9b)	119.4 (7)	N(2b)-C(3b)-C(4b)	117.8 (9)
C(9b)-C(3b)-C(4b)	122.8 (8)	C(3b)-C(4b)-C(5b)	120.8 (9)
C(4b)-C(5b)-C(6b)	119.7 (10)	C(5b)-C(6b)-C(7b)	120.8 (9)
N(2b)-C(7b)-C(6b)	118.8 (8)	N(2b)-C(7b)-C(8b)	116.8 (7)
C(6b)-C(7b)-C(8b)	124.0 (8)		

away from the center point). The lutidine rings of the two axial 2,6-lutidine *N*-oxide ligands appear to be oriented in a random manner with respect to one another and with respect to the porphyrin ring. For example, the torsion angles defined by atoms O(1a)-Mn-O(1b)-N(2b) is −135.8° and that defined by atoms O(1b)-Mn-O(1a)-N(2a) is −145.6°. One lutidine ring makes an angle of 44.3° with the mean N_4 plane; the other makes an angle of 39.6° with this plane. The orientation of the lutidine rings can best be attributed to crystal-packing forces whereas the nonpolanarity of the porphyrin ring must be attributed to both crystal-packing forces and the size and electronic structure of the manganese atom.

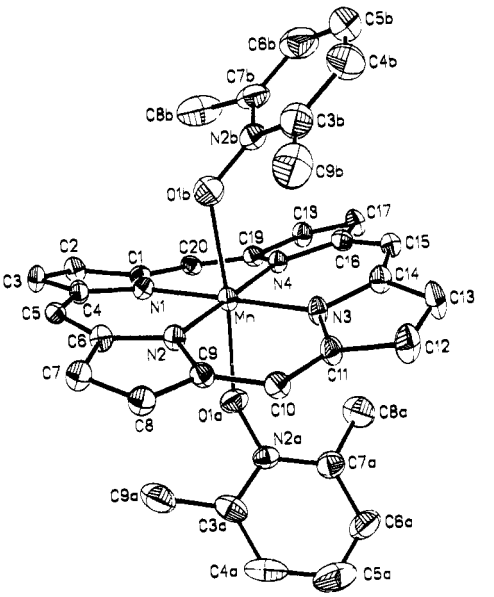

Figure 4. ORTEP[33] and numbering diagram for the bis(2,6-lutidine *N*-oxide)(tetraphenylporphinato)manganese(III) cation of **1**. The perchlorate counterion and the heptane molecule of crystallization along with the cation protons and the porphyrin phenyl carbons have all been omitted for clarity. The thermal ellipsoids represent the 30% probability surface.

Selected bond distances and angles are summarized in Tables III and IV, respectively. The Mn-to-N(porphyrin) distances, $d_{Mn-N(Por)}$, in **1** of 1.999 (4), 2.004 (4), and 1.991 (4) Å (two of them) are typical of those for $S = 2$ Mn^{III} porphyrin complexes[15] and more generally for first-row transition-metal metalloporphyrin complexes where the σ-antibonding $d_{x^2-y^2}$ orbital is unoccupied.[34] The angle defined by the axial oxygen atoms and the manganese atom, O1a-Mn-O1b, is 173.2 (2)°. The origin of the deviation of this angle from 180° is uncertain although it is clear that it does not arise from steric interaction of the lutidine methyl groups with the porphyrin ring. An analysis of the closest contacts in the unit cell of **1** shows that there are no intramolecular nonbonding interactions in the bis(2,6-lutidine *N*-oxide)(tetraphenylporphinato)manganese(III) cation that are sterically significant.

The interesting bond distances d_{M-O} and d_{O-N} and the interesting angle M-O-N of **1** and other complexes containing terminal aromatic amine *N*-oxide ligands are summarized in Table V. Three features are obvious upon examination of the data in Table

Table V. Structural Data on Representative Aromatic Amine *N*-Oxide Complexes[a]

metal complexes[b]	*R* of structure, %	d_{M-O}	d_{O-N}	M-O-N angle	ref
$[Mn^{III}TPP(2,6\text{-lutNO})_2]^+ClO_4^-$ (**1**)	9.1	2.263 (4)	1.331 (7)	128.8 (3)	this work
		2.264 (4)	1.330 (6)	126.5 (3)	
First-Row Transition-Metal Complexes with Terminal *N*-Oxide Ligands					
$Cu^{II}(pyrNO)_2(NO_3)_2$	7.5	1.968 (5)	1.362 (7)	118.6	35
		1.951 (5)	1.361 (7)	119.4	
$Cu^{II}(pyrNO)_4(ClO_4)_2$	10.4	1.93	1.34 (1)	116.7 (7)	36
		1.92	1.33 (1)	118.7 (6)	
$Cu^{II}(2,6\text{-lutNO})_2Cl_2$	8.3	1.97 (1)	1.31 (1)	118.6 (9)	37
		1.93 (1)	1.36 (1)	121.6 (9)	
$Zn^{II}(2,6\text{-lutNO})_2Cl_2$	11.6	2.01 (1)	1.35 (3)	118.6 (7)	38
$Ni^{II}(pyrNO)_2(acac)_2$	9.7	2.105 (5)	1.337 (6)	122.4 (4)	39
		2.088 (5)	1.321 (9)	119.2 (4)	
Main-Group Metal Complex with Terminal *N*-Oxide Ligands					
$Sn^{IV}Cl_2Me_2(pyrNO)_2$	9.2	2.25 (2)	1.37 (2)	117 (1)	40

[a] Distances in angstroms; angles in degrees. [b] For abbreviations, see ref 12.

V. First, the Mn–O bond distance in **1** is 0.2–0.3 Å longer than in similar complexes of first-row transition metals. In addition, the structurally characterized high-spin ferric complex [Fe(TMSO)$_2$TPP]$^+$ClO$_4^-$, TMSO = tetramethylene sulfoxide, of Scheidt and Reed contains a trivalent first-row transition metal axially ligated to a neutral oxygen atom of hybridization similar to that of the oxygen of 2,6-lutidine *N*-oxide. The axial Fe–O distances in this complex are 2.069 (3) and 2.087 (3) Å, and although these distances are longer than other Fe^{III}–O bond distances, they are substantially shorter than the Mn^{III}–O bond distances in **1**. Most of this tetragonal elongation of the bonds to the axial oxygens in **1** can be attributed to a singly occupied axially antibonding d_{z^2} orbital and confirms a ground electronic state for the Mn^{III} atom of $(d_{xz}\pi, d_{yz}\pi)^2(d_{xy})^1(d_{z^2}\sigma)^1$. Second, the N–O bond lengths in the axial 2,6-lutidine *N*-oxide ligands of **1** are not greatly different from these bond lengths observed in the other complexes. Indeed, the entire range of N–O bond lengths for the complexes in Table V is 1.31 (1)–1.37 (2) Å with those of **1** being 1.330 (6) and 1.331 (7) Å. The conclusion from this coupled with the reasonable thermal stability of the isolated complex **1** is that the N–O bonds in **1** are not strongly activated electronically with respect to heterolytic cleavage to yield the formal oxomanganese(V) species and lutidine nor to homolytic cleavage to yield a formal oxomanganese(IV) species and lutidine cation radical, eq 1 and 2, respectively. The third and final feature

$$[L(Por)Mn^{III}\leftarrow O—NR]^+ \rightarrow [L(Por)Mn^{V}{=}O]^+ + NR \quad (1)$$

$$[L(Por)Mn^{III}\leftarrow O—NR]^+ \rightarrow L(Por)Mn^{IV}{=}O + NR^+\cdot \quad (2)$$

worthy of comment is the angle defined by the metal atom and the oxygen and nitrogen atoms of the *N*-oxide ligands in the complexes enumerated in Table V. These angles, including those for 1, all fall within the narrow range of 117–128°. Since few of the aromatic *N*-oxide ligands are sterically encumbered by neighboring ligands or intermolecular solid-state interactions in these complexes, one might use the simple valence-bond formalism and attribute the M–O–N angles in part to M–O bonding involving orbitals residing primarily on oxygens that are largely sp^2 hybrid in nature.

Acknowledgment. Support of this work by the National Science Foundation (Grant No. CHE-8402994) is acknowledged.

Registry No. **1**·C$_7$H$_{16}$, 97073-98-8; **1**, 97073-97-7; Mn^{III}TPP(ClO$_4$), 79408-54-1.

Supplementary Material Available: Crystallographic data for **1** including anisotropic temperature factors (Table SVI), hydrogen coordinates and temperature factors (Table SVII), observed and calculated structure factors (Table SVIII), nonbonded distances and torsion angles (Table SIX), nonessential bond distances and angles (Table SX), an ORTEP plot of **1**, and a stereoview of the crystal packing diagram for **1** (52 pages). Ordering information is given on any current masthead page.

Contribution from the Department of Chemistry,
Purdue University, West Lafayette, Indiana 47907

Optical and Thermodynamic Basicities: UV Spectra of Tl^+, Pb^{2+}, and Bi^{3+} in Molten Chloroaluminate Titrations

P. D. BENNETT* and C. A. ANGELL

Received August 1, 1984

Following a recent report on the strong environmental dependence of the $^3P_1 \leftarrow {}^1S_0$ transition of Pb^{2+} doped, in trace quantities, into thermodynamically characterized binary chloroaluminate molten-salt systems, we examined two other isoelectronic ions, Tl^+ and Bi^{3+}, in order to gain insight into the factors determining a spectral probe's sensitivity to chemical processes and into the limitations of the use of $d^{10}s^2$ ions as basicity probes. Major differences in the probe ion spectral responses ranging from full-range frequency shifts (Bi^{3+}) to no shift at all (Tl^+) were observed as their host solvent was titrated through a composition region where large thermodynamic changes are known to occur (equivalence point at the $AlCl_4^-$ stoichiometry). These differences are discussed in terms of differences in the polarizing power of the probe ions and the ions composing the solvent medium, and in terms of probe ion coordination symmetries and stoichiometries.

Introduction

The ultraviolet absorption spectrum of $d^{10}s^2$ ions doped, in trace quantities, into molten salts,[1-8] crystals,[9-10] and glasses[3-6,11-25] has been the subject of many publications. Interest has focused on the strong environmental dependence of the outer-orbital $^3P_1 \leftarrow {}^1S_0$ transition ("Rydberg") characteristic of $5d^{10}6s^2$ ions; in particular, the frequency dependence of this transition for Tl^+, Pb^{2+}, or Bi^{3+} on composition changes in the molten or glassy solvent has been of prime concern. For example, the spectrum of the dopant, or probe ion, exhibits progressive shifts to the lower energy region of the UV spectrum as the (Lewis) basicity of the solvent is increased, both by increasing the concentration of the more basic component within a single system (e.g., increasing the concentration of Na_2O in B_2O_3/Na_2O glass) and by going to stronger bases in a given solvent system (e.g., going from B_2O_3/Na_2O to B_2O_3/K_2O glasses[3]).

These observations were interpreted in terms of the unusual sensitivity of the probe ions to the electron-donating propensity of their first nearest neighbors. The acid strength, or polarizing power, of the probe ion's second nearest neighbors determines the

* To whom correspondence should be addressed at the Electrochemical Energy Storage Group, Standard Oil (Ohio) Research Center, Cleveland, OH 44128.

(1) C. A. Angell and P. D. Bennett, *J. Am. Chem. Soc.*, **104**, 6304 (1982).
(2) G. P. Smith, D. W. James, and C. R. Boston, *J. Chem. Phys.*, **42**, 2249 (1965).
(3) J. A. Duffy and M. D. Ingram, *J. Am. Chem. Soc.*, **93**, 6448 (1971).
(4) J. A. Duffy and M. D. Ingram. *J. Inorg. Nucl. Chem.*, **36**, 39 (1974).
(5) J. A. Duffy and M. D. Ingram. *J. Inorg. Nucl. Chem.*, **36**, 43 (1974).
(6) J. A. Duffy and M. D. Ingram, *J. Inorg. Nucl. Chem.*, **37**, 1203 (1975).
(7) H. Suito and R. Inove, *Trans. Iron Steel Inst. Jpn.*, **24**, 47 (1984).
(8) D. R. Gaskell, *Trans. Iron Steel Inst. Jpn.*, **22**, 997 (1982).
(9) F. Seitz, *J. Chem. Phys.*, **6**, 150 (1938).
(10) D. S. McClure, *Solid State Phys.*, **9**, 512 (1959).
(11) A. K. Ghosh, *J. Chem. Phys.*, **42**, 2623 (1964); **44**, 535 (1966).
(12) R. Reisfeld, *Struct. Bonding (Berlin)*, **13**, 53 (1973).
(13) R. Reisfeld and L. Boehm, *J. Non-Cryst. Solids*, **16**, 83 (1974).
(14) R. Reisfeld and L. Boehm, *J. Non-Cryst. Solids*, **17**, 209 (1975).
(15) J. A. Duffy and M. D. Ingram, *J. Chem. Soc. A*, 451 (1970).
(16) J. A. Duffy and M. D. Ingram, *J. Chem. Phys.*, **52**, 3752 (1970); **54**, 443 (1971).
(17) J. A. Duffy and M. D. Ingram, *Phys. Chem. Glasses*, **16**, 124 (1975).
(18) R. Klein and P. I. K. Onorato, *Phys. Chem. Glasses*, **21**, 199 (1980).
(19) A. Paul, *Phys. Chem. Glasses*, **11**, 46 (1970); **13**, 144 (1972).
(20) A. J. Easteal and A. T. Morcom, *J. Non-Cryst. Solids*, **34**, 29 (1979).
(21) A. J. Easteal and D. J. Udy, *Phys. Chem. Glasses*, **14**, 107 (1973).
(22) S. Sumita, Y. Matsumoto, K. Morinagra, and T. Yanagase, *Trans. Jpn. Inst. Met.*, **23**, 360 (1982).

0020-1669/85/1324-3030$01.50/0